Received: 24 March 2021 | Revised: 22 May 2021 | Accepted: 23 May 2021

DOI: 10.1002/app.51215

ARTICLE

Journal of Applied Polymer Science WILEY

Structural description of self-reinforced polypropylene composites

Angela Ries

Faculty of Engineering and Mathematics, Bielefeld University of Applied Sciences, Bielefeld, Germany

Correspondence
Angela Ries, Faculty of Engineering and Mathematics, Bielefeld University of Applied Sciences, 33619 Bielefeld, Germany.
Email: angela.ries@fh-bielefeld.de

Abstract

Self-reinforced polypropylene composites (SR-PP) possess an exceptional property spectrum and are predestined for use in a multitude of structural or semi-structural applications. However, the underlying macromolecular orientation can only be transferred into the layered composites consolidated out of highly stretched fibres and tapes of semi-finished textile products. Specific preservation of the self-reinforcement throughout processing and beyond is necessary and creates special challenges for processing technology. Depending on the processing temperatures and pressures selected, the highly oriented fibres and tapes are influenced by their own degree of self-reinforcement, which, in turn, affects the microstructure and remaining composite properties. In this publication, three different semi-finished textile products are introduced as basic materials. Exemplary selected test samples, which display a low degree of compaction on the one hand and a high degree of compaction on the other, were subject to wet chemical etching to enable confocal laser scanning microscopic images to be created. These images were then used to compare the microstructures of the semi-finished textile products that were used.

1 | INTRODUCTION

Self-reinforced thermoplastic composites have immense potential for lightweight application and display excellent mechanical properties.[1] Their reinforcement is solely based on the self-reinforcement of the polymer itself that is implemented by melt and solid phase deformation.[2] By means of this particular orientation of the crystalline areas, excellent basic properties of the polymer in the direction of orientation can be obtained.[3–5] However, the mechanisms of self-reinforcement are difficult to implement directly into complex structural components, making an intermediate step involving semi-finished textile products necessary. More precisely, the above-mentioned melt and solid phase deformations can be carried out most efficiently on semi-finished textile products, such as woven or non-woven fabrics or fleeces.[6–10]

The semi-finished textile products are then layered and hot-compacted into laminates by applying heat and pressure.[11,12] During the manufacturing of these composites, the oriented polymer sections are embedded in an identical polymer matrix. Thus, self-reinforced polypropylene (SR-PP) fibre composites are an intelligent combination of highly oriented polymer material and a structural composite.[13] They are not comparable to conventional composite materials, which consist of two different phases from two differing chemical sources. In the case of SR-PP composites, added value is incorporated into the component based on the macromolecular orientations without integrating conventional foreign fibres for reinforcement that are based on glass fibres, carbon

fibres, aramid fibres or natural fibres. They display excellent recyclability owing to the fact that they consist of a single material system. The properties of these self-reinforced composites are up to four times higher when it comes to stiffness and five times higher in regard to strength compared to compact PP. They can easily compete with glass fibre reinforced polypropylenes.[14]

Another benefit of this material concept is that it is the foundation for exceptionally high impact strength and puncture resistance (that increases at the lowest temperatures). The reason for this simply lies within the particularly beneficial absorption and transformation of energy. The layered composite itself displays delamination with low damage,[7,15–17] which is additionally fostered by the ductility of the polypropylene.[18] In contrast to conventional thermoplastic composites, the material does not become brittle at low temperatures; brittleness would normally induce fracturing or splintering when the material is subject to impact.[5,19] This is due to the fact that the endless fibres (tape fabrics) and fibre filaments (fleeces) fibrillate when subject to large amounts of deformation. Subordinate to this, tape/fibre pull-outs and fractures occur. In the automobile industry in particular, possibilities for technical implementation exist to replace glass fibre reinforced components (i.e., made of glass mat reinforced thermoplastic [GMT]) with self-reinforced PP components. Especially suitable product groups are very large semi-structural components, which are subject to high impact and are not exposed to a high temperature.[20] For example, this applies for underbody panelling and loading areas.[4] Thanks to their balanced property profile, component thicknesses can be reduced by 20% to 30% without any issue according to Klimke.[5] Moreover, the density-related weight reduction by approximately 30% in comparison to conventional glass fibre reinforced PP ($\rho_{PP\text{-}GF30} = 1.18\ g/cm^3$ vs. $\rho_{SR\text{-}PP} = 0.91\ g/cm^3$) is also advantageous for the overall outcome, making it easy to achieve weight reductions by up to 50% while maintaining the same properties.[5,21]

The following list shows the application fields in which self-reinforced PP composites have already become established. The product assortment ranges from simple, large and lightly reshaped panelling components to applications subject to shock and impact (impact and shock-resistant knee protectors, ice skates), as well as large components in series application (for example, extremely lightweight suitcases from the Cosmolite series by Samsonite).[14]

The correct selection of semi-finished textile products already determines the physical and mechanical variables of the later layered composites. The selection of the semi-finished textile products is made based on the criteria textile type and bonding type as well as surface weight (regulate laminate thickness by the layer count) and matrix selection. In most cases, self-reinforced fibre composite materials consist of highly oriented semi-finished PP textile products (e.g., PURE, Curv, PARALITE, and Armorodon).[22] Polyethylene, polyethylene terephthalate or polyamide-based semi-finished textile products are used less often, even though they are commercially available (PE = Kaypla; PET = Comfil).[22]

Despite all these benefits, the self-reinforcement is extremely sensitive to temperature and pressure during processing. The slightest parameter changes during processing can affect the later composite properties permanently. This disadvantage is especially bothersome when unwanted, different processing temperatures and/or pressures are present in the tool during processing, and result in undesired effects on the components. Then again, these effects of self-reinforced material systems can be used for a strong gradation potential.[14] During thermal gradation, the thermoplastic fibres and tapes are melted to varying degrees by means of directed, locally effective temperature differences of the heating and/or cooling rates across the tool surface in the pressing process and/or pre-heating sequence in order to vary the structural properties sustainably. Additionally, increasing the pressure used to perform pressing locally, so-called mechanical gradation, promotes better compaction due to increased heat conduction and an elevated degree of melting in the tapes or fibres.[14]

In order to describe the gradation potential, this study focused on a hot compaction process with two differing process parameters, which depict a relatively low and high degree of compaction of self-reinforced polypropylene composites. The goal of the structural analysis was to describe the specific material composition defined by the semi-finished textile products used and to characterise and compare the morphology of self-reinforced fibre composite materials based on the low and high degrees of compaction achieved with varying process parameters. In the following examinations, the structural analysis was carried out using confocal laser light microscopy, which involves reflected light on a sample surfaces that has been treated with wet chemical etching.

Scanning electron microscopy (SEM) may impress with higher resolutions ranging from 1 to 2 nm (depending on the sample being examined, even significantly smaller), but has the disadvantage that it requires extensive preparation methods, such as vaporization, so-called sputtering of non-conductive surfaces, except for low vacuum scanning electron microscopy. In particular, sputtering with a very thin layer of precious metal (e.g., gold) or with a carbon layer (graphite) can prove to be very problematic when dealing with sensitive self-reinforced polypropylene composites. During sputtering—more precisely, cathode sputtering—atoms are separated out of a solid body by specifically firing with ions and then transition into the gaseous phase.[23] This then precipitates on the sample as a fine layer.[23] The energy of the ions needed, however, changes the highly oriented

TABLE 1 Basic properties of the employed textile materials[24–26]

Product name	Unit	Test method	SNW17	SG30/30	Pure
Material system	(−)		Needle-punched staple fibre fleece	Mono-extruded 2/1 Twill fabric	Co-extruded canvas fabric
Tensile strength MD/CD	(kN/m)	EN ISO 10319	9.8/10.5	30.0/30.0	
Tensile strength	(MPa)	ISO 527			500
Maximum stretching MD/CD	(%)	EN ISO 10319	50.0/50.0	20.0/11.0	
Maximum stretching MD/CD	(%)	ISO 527			6.0 / 6.0
Fibre length/diameter tape width/thickness	(mm/µm)		N/A/20	2.6 MD, 1.3 CD/60	2.2/70
Surface weight	(g/m^2)		150	124	105
Number of layers in composite	(−)		12	16	16

Abbreviations: CD, cross direction; MD, machine direction.

structures of the self-reinforced samples, even destroys them. For this reason, classic SEM—which was available in the context of these examinations—was decidedly ruled out for assessing the self-reinforced composite structures.

2 | COMPOSITE MANUFACTURE

2.1 | Basic textile materials

There is an extensive selection of semi-finished textile products based on polypropylene available for the consolidation of self-reinforced composites. Three textiles were selected in the context of these examinations. They differ from one another in regards to their morphology (monoextrudate, coextrudate) and textile type (staple fibre fleece, tape fabric), and enable comparisons to be made regarding their material-specific process structure correlations. In the following chapters, the semi-finished textile products will be introduced individually and then summarized in Table 1.

Both geotextiles (SNW17 and SG30/30) used here only consist of a uniform polymer structure and are, therefore, classified as monoextrudates. These material systems display exceptionally high process sensitivity. A coextruded tape fabric by the product name Pure was added as a counterpart, its morphology only prevents the process parameters from having much influence. An additional criterion for textile selection was the assurance of conventional availability of the products in order to be able to guarantee their availability for the industrial manufacture of self-reinforced composites as well.

2.1.1 | Needle-punched staple fibre fleece SNW17

The needle-punched staple fibre fleece SNW17 is a white geotextile made by the company Bonar from Belgium, and is based on polypropylene (Figure 1). The product name is derived from the title "sheet non-woven" and the static puncture resistance (CBR) equalling 1.7 kN.[24] The fibres consist of thin, oriented endless polypropylene filaments with a diameter of maximally 20 µm. The fixation of the endless fibres in the direction of thickness was carried out with a tempered needle roller, enabling simple handling and draping of the fleece system. Moreover, the fleece possesses a marked isotropy owing to its random orientation and layered endless fibres, which makes the manufacture of self-reinforced composites independent of their orientation possible.

2.1.2 | Mono-extruded twill fabric SG30/30

Another semi-finished textile product used that is based on monoextrudates was the 2/1 twill fabric SG30/30 (Figure 2). Its product name is derived from the abbreviation for "standard graded" and a tensile strength of 30.0 kN/m in MD and CD.[25] This black fabric consisting of highly stretched polypropylene film tapes is also a geotextile made by the company Bonar from Belgium.

The classic 0°/90° anisotropy of this textile results from the selected 2/1 twill weave. Two tapes with a cross-sectional width of 1.3 mm (0°) run into one tape with a cross-sectional width of 2.6 mm (90°) and wrap around it. SG30/30 can be draped excellently owing to its type of weave. The only disadvantage is the increased number of pulled out tapes in the marginal area due to high ondulation when cutting the textiles. This is due to the twill weave and has no consequences for the later composite and its properties.

2.1.3 | Co-extruded canvas fabric pure

The co-extruded tape fabric Pure manufactured by the company Lankhorst, Netherlands, which is based on

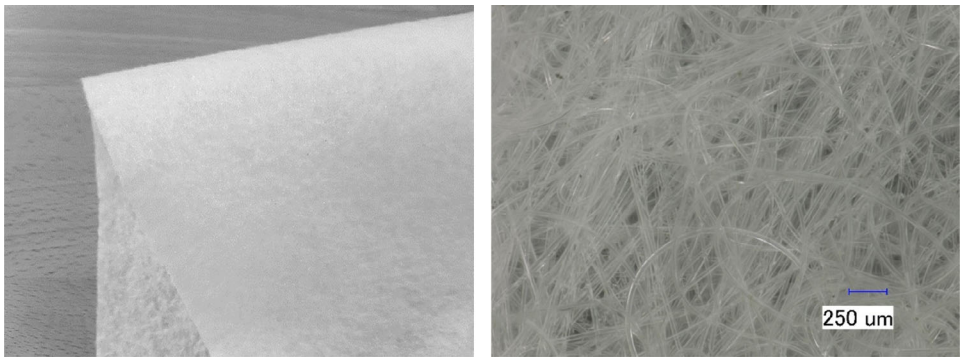

FIGURE 1 Left: SNW17 needle-punched staple fleece fibre; Right: ×100 magnification of an SNW17 textile layer [Color figure can be viewed at wileyonlinelibrary.com]

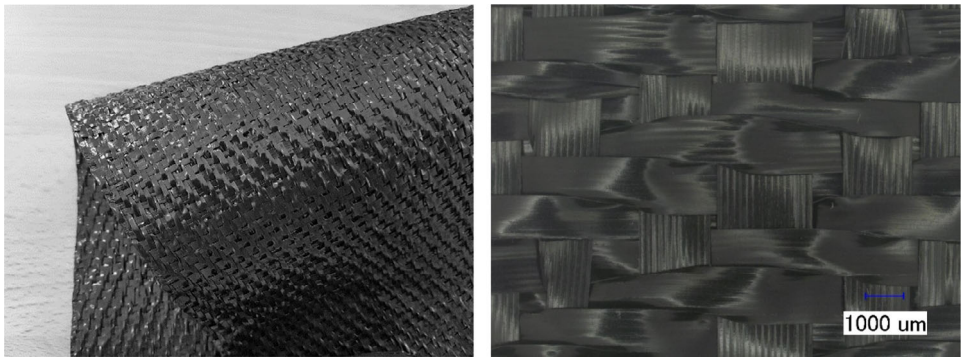

FIGURE 2 Left: SG30/30 twill weave; Right: ×20 magnification of an SG30/30 textile layer [Color figure can be viewed at wileyonlinelibrary.com]

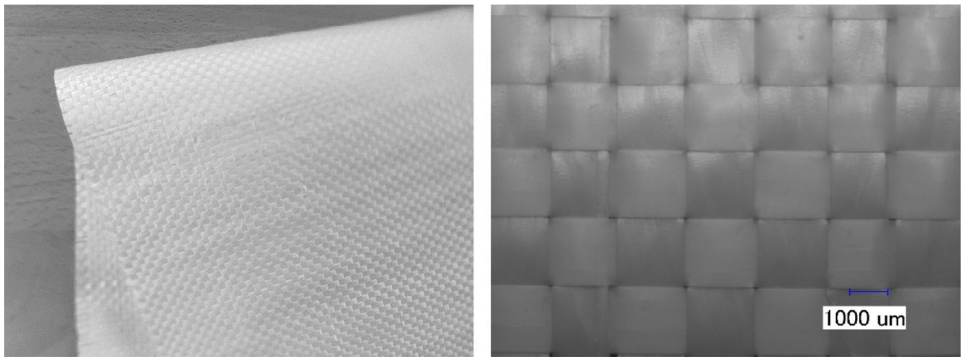

FIGURE 3 Left: Pure tape fabric with recognizable weaving errors due to folded and creased tapes; Right: ×20 magnification of a Pure textile layer [Color figure can be viewed at wileyonlinelibrary.com]

polypropylene, was one of the semi-finished textile products used in this study. The highly oriented tapes have a cross-sectional width of 2–2.2 mm, a thickness of 70 µm, and are combined in a plain weave. The tapes have marginally extruded outer layers consisting of a co-polymer with a lower melting point than the inner core layer of polypropylene. Since this is a conventional product, detailed material information regarding the core and surface layers is not available for competitive reasons on the manufacturer's part. When generating a matrix, the outer surface layers can be melted without the highly oriented polymer phase losing its highly oriented textures, meaning without affecting its superior mechanical properties, respectively. The tensile strength of the tapes equals 500 (N/mm^2).[26] Even though it can be assumed that there are weaving errors in the consolidated composite in form of folded tapes (Figure 3), this high-performance fabric is specifically characterized by its reproducibility.

2.2 | Hot compaction process

A total of 12 layers of the staple fibre fleece system SNW17 or 16 layers of the tape fabric SG30/30 or Pure were layered in a clamping frame and hot compacted into approximately 2 mm thick laminates by applying heat and pressure. The consolidation of the semi-finished textile products into plate-shaped laminates with the dimensions $500 \times 500 \times 2\ mm^3$ was carried out in a hot compaction process using the two processing parameters series A and B specified in Table 2 on an 800 kN precision laboratory press of the company Gottfried Joos Maschinenfabrik GmbH & Co. KG. Prior to the actual hot

TABLE 2 Processing parameters of the exemplary, selected samples according to manufacturing processes A and B for the structural description using CLSM

	IR pre-heating sequence		Hot compaction process		
Process	IR temperature T_{IR} (°C)	IR pre-heating time t_{IR} (s)	Temperature T (°C)	Pressing time t_p (s)	Pressure p (MPa)
A	155	121	174	175	3.0
B	120	192	183	100	1.8

compaction process, an IR pre-heating sequence was completed to temper the semi-finished textile products homogeneously. After the pre-heating sequence, the clamping frame containing the semi-finished textile products was transferred to the pressing unit pneumatically, where the hot compaction process was then completed with the selected parameters for temperature, time and pressure. The subsequent cooling sequence was carried out isostatically at a constant hot compaction pressure for 600 s, in order to cool the panel-shaped laminate for removal at room temperature.

The process parameters A and B were determined while taking numerous pre-test screenings into account and represent low and high compaction degrees. Prior processing attempts for manufacturing thermo-mechanically graded, layered composites were carried out according to the Latin Hypercube Design (LHD) with an experimental scope of n = 16 processing series.[14] LHD is characterized by an experimental scope that can be set as desired and the possibility to make substantiated statements about the testing room and the assessment of interactions between the individual process parameters owing to the systematic, room-filling setup even after only a few tested points.[27] The subsequent mechanical composite characterization of the manufactured SR-PP composites was carried out in numerous quasi-static tensile and 3-point bending tests, as well as a 10 J impact test. Thus, a dependable correlation of the interactions between the process and properties exists.[14] The composite properties are decisively influenced by the pressing temperature T_P, the compaction pressure p and the pressing time t_P. Moreover, they are also influenced by the IR pre-heating sequence with the IR temperature T_{IR} and IR pre-heating time t_{IR}. The selection of the process parameters can result in them influencing each other strongly. For example, they cannot fall short of a specific compaction temperature in order for sufficient melt phase. This is necessary to be able to be generated to ensure the required intralaminar composite adhesive strength in which the still highly oriented structures are embedded. If the process temperature is too high instead, the macromolecular orientations are overheated, resulting in a loss of the self-reinforcement. The effects named here in addition to the temperature are also dependent on the exposure time in the IR pre-heating sequence t_{IR} and pressing phase t_P.[14]

In addition to the time-dependent temperature strain, the influence of the compaction strength during the consolidation phase also contributes to the further, crucial influencing of the properties. The level of compaction pressure affects the flow mechanisms of the polymer.[28] In particular, the matrix percolation and melt flow process are strongly influenced by this and display a direct effect on the later composite properties.[28] Moreover, it is important to note that a generally higher compaction pressure improves heat conduction in the textile stack, which is expressed in form of a higher degree of melting of the fleece fibres or tape fabrics.[21] Depending on the semi-finished textile product used (monoextrudate vs. coextrudate and fibres vs. tapes), the strengths of the effects vary considerably.[14] The process parameters A and B selected here represent a low and high compaction degree in this case, which takes the previously mentioned tension fields into account, even regarding the three different semi-finished textile products used here.

2.3 | Preprocessing samples

In order to be able to perform a morphological examination of the composite laminates with the dimensions 500 × 500 mm², the workable samples were subject to basic machining initially. Afterward, the Bühler low speed precision separator IsoMet 4000 was used to carry out precise machining to create microscopy samples with the dimensions 15 × 20 mm². Here, low rotation counts equalling 200 rpm, small advancements by 2 mm/min in combination with cooling with water were utilized to keep the thermic effect on the samples as low as possible and to inhibit the correlating effect on the structure.

3 | PERFORMING THE STRUCTURAL ANALYSIS

The description of the structure of self-reinforced polypropylene composites was carried out for the types of

samples that had a relatively low and a relatively high degree of compaction. The samples which had been prepared as reflected light microscopy samples were analysed after wet chemical etching. Confocal laser scanning microscopy was employed and the samples were compared. Not only were the degrees of compaction compared, but also the utilized semi-finished textile products amongst one another. In the following chapters, the microscopic method and the sample preparation with wet chemical etching will be described in detail.

3.1 | Confocal laser scanning microscopy

In contrast to conventional light microscopy, confocal laser scanning microscopy (CLSM) can produce a significantly higher resolution.[29] The Lext OLS3100 and the according surface texture analysis software made by Olympus were used for these examinations.[30] Instead of using a conventional light source with a wavelength of approximately 500 nm, CLSM uses a laser diode with a wavelength of approximately 408 nm, thus achieving much finer surface and depth resolution in the microscopic imaging of up to 1 μm.[31,32] Owing to this resolution capacity, CLMS can be used in additional application fields which were previously only reserved for electron optic measurement methods, like for example the scanning electron microscope (SEM).[32]

3.2 | Sample preparation

The samples preprocessed with the low-speed precision separator and measuring $15 \times 20\ mm^2$ were sanded by hand in a sanding processes with multiple steps. Silicon carbide sandpapers with increasingly finer grits (600, 1200, 2500, and 4000) were used. Cooling in water encompassed cooling, lubrication, and rinsing off abrasively removed particles from the workspace. After completing each sanding step, the samples were cleaned in an ultrasonic bath in de-ionized water to remove remnant particles from sanding from the surface. Final polishing of the sanded surface was foregone in order to ensure the sample surfaces still retained their remaining roughness before they were put through the ensuing wet chemical etching process.

3.3 | Wet chemical etching of self-reinforced PP composite structures

In order to contrast the different polymer phases using reflected light microscopy, a prior wet chemical etching process is needed which increases the visibility of the oriented structures on the sample surfaces to be examined.

First, the etching solution removes the amorphous phases on the semi-crystalline thermoplastics, exposing the crystalline phases and their superstructures.[33] Only very aggressive wet chemical media are suitable for non-polar, carbon-based iso chains—like those present in polypropylene.[34]

The etching rate v_e (mg/mm^2s) describes the standardized removal in form of loss of mass m_v (mg) on the (sample surface) area A (mm^2) throughout the duration of exposure or the etching time t_e (s).

$$v_e = \frac{m_v}{A^* t_e} \tag{1}$$

The quality of the etching result and correlating control thereof using the etching rate are fundamentally dependent on the etching solution used, its concentration, temperature when used, and the required etching time.[33] Using polyethylene as an example, the research group led by Bashir et al. was able to verify that highly crystallized structures require significantly longer etching times than classic spherulitic structures.[35] Analogous to the particularly highly oriented (self-reinforced) polypropylenes, it is important to take an adjusted exposure duration into account. The ideal etching time was determined to be 2 to 5 days at room temperature.[36]

In order to expose the fine structure to be able to examine the arrangement of the lamellae, permanganate etching with 0.7% dissolved potassium permanganate ($KMnO_4$) in a 2:1 mixture of concentrated sulfuric acid (H_2SO_4) and orthophosphoric acid (H_3PO_4) established itself as the most promising option,[34,37–39] see Table 3.

The previously used, highly toxic potassium dichromatic sulfuric acid solution ($K_2Cr_2O_7$: H_2O: H_2SO_4 with 4.4: 7.1: 8.1 weight ratios) has been replaced by this more advanced etching solution in the meanwhile.[40]

To start the solution, 70 ml of orthophosphoric acid are poured into a beaker, and 140 ml of sulfuric acid are added while stirring with a magnetic stirrer.[14] The acidic solution is subsequently cooled in a water bath with ice cubes while powder potassium permanganate is added gradually.[14] The latter gives the freshly mixed solution a dark green colour. Throughout the exposure period, the solution reduces, turning violet as the effect wears off. Olley even observed that the etching speed increased by adding water to the started permanganate solution and rougher surfaces were visible on the sample.[34,37] This modification was not examined further in the context of the examinations.

As previously mentioned, the exposed etching time t_e extends over a period of 2 to 5 days depending on the sample used. After completing the etching process, a

TABLE 3 Composition of the 210 ml permanganate etching solution for contrasting self-reinforced polypropylene composites[14]

Etching medium	Molecular formula	Concentration	Quantity	Aggregate state	Color	
Phosphoric acid	H_3PO_4	96%, undiluted	70 ml	Liquid	Clear, colorless	Dark green in solution
Sulfuric acid	H_2SO_4	98%, undiluted	140 ml	Liquid	Clear, colorless	
Potassium permanganate	$KMnO_4$	100%, pure form	1.47 g	Solid	Black	

TABLE 4 Rinsing media for treatment of the sample after etching with permanganate[14]

Step	Subsequent treatment	Molecular formula	Concentration	Aggregate state	Color
1	Sulfuric acid	H_2SO_4	98%, 2:7 diluted	Liquid	Clear, colorless
2	Hydrogen peroxide	H_2O_2	30%	Liquid	Clear, colorless
3	Ethanol	C_2H_6O	98%, undiluted	Liquid	Clear, colorless

Note: Prof. Dr.-Ing. Angela Ries has been a professor at Bielefeld University of Applied Sciences since September 2020 and works in the field of plastics technology and lightweight construction. From September 2017 to August 2020 Ms. Ries was junior professor and head of the Heterogeneous Materials Group at the Institute of Materials Engineering at the University of Kassel, Germany.

termination reaction of the etching process is carried out by completing multiple consecutive rinsing processes, initially with 2:7 diluted sulfuric acid (final concentration of 21.8%) and then with a de-ionized water and hydrogen peroxide mixture, see Table 4. The final washing procedure of the sample is carried out in an ultrasonic bath with ethanol and drying is completed with compressed air.[14]

4 | STRUCTURAL DESCRIPTION

The wet chemical etching process removed the amorphous phase.[33] This is visible in the exposed differences in height on the sample surface when using the confocal laser scanning microscope and, unlike polarized transmitted light microscopy, enables a comparably plastic presentation of the highly stretched structures.

A comparison of the reflected light microscopy images of selected sections of the composite cross sections of the various textile systems is provided in the following subchapters using two selected, exemplary process parameters (Table 3) from process series A (low compaction temperature, long pressing time, medium pressure level) and process series B (high compaction temperature, short pressing time, low pressure level).

4.1 | Structural description of composites made of needle-punched staple fibre fleece SNW17

The layered composites based on the staple fibre fleece SNW17 displayed individual fibre filaments with unmistakable, fibre-shaped to ellipsoid structures in the detailed images shown in Figure 4. These structures result from the specific, isotropic fibre orientations, which display according different longitudinal, orthogonal or oblique cut surfaces. Depending on the varying fibre orientations, differing degrees of highly oriented fine structures can be identified by their characteristic textural differences. In the incident light images of the SNW17 fibre fleece composites manufactured according to process A, a flatter surface topology was visible in comparison to those made with process B. Samples manufactured according to process B, in contrast, displayed a compacter, more closed surface topology. This causes the more starkly contrasted height differences of the textural structures in the fibre cuts to be significantly more visible. However, we decided not to continue to measure these and make deductions about the degree of orientation. It can be assumed that the contrasts set during incident light microscopy can differ mildly from one another and this, in turn, could falsify a direct comparability of the quantitative measurement points.

When comparing the low compaction temperature process A and the higher consolidated process B, a difference in the packing density of the fleece-type cavities is visible. For example, samples manufactured according to process A have cone-shaped areas of trapped air in the intersecting points of fibres situated transverse to one another in comparison to samples manufactured according to process B. However, what is substantially more noticeable is a deep-set, crater-like enclosure of air in the right section of the microscopy image of the sample made with process A. This enclosure of air exposes the surface structure of the fibre filaments. This observation makes it possible to deduct that the degree of

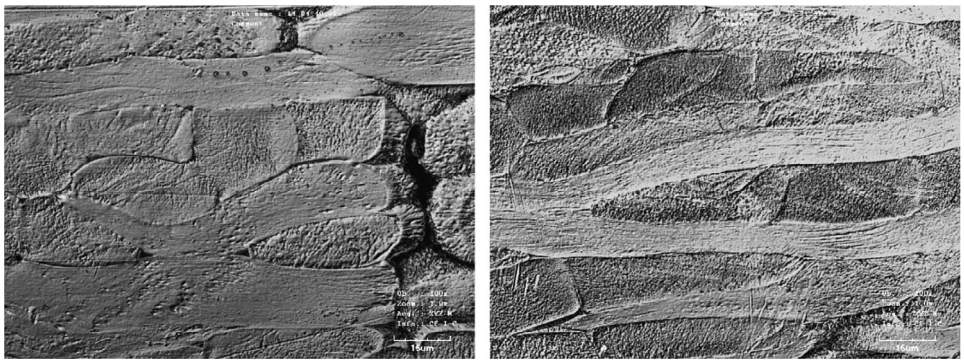

FIGURE 4 Detailed reflected light images of the CLSM with ×1000 magnification of wet chemically etched, self-reinforced composites structures made of SNW17 according to the process parameters A (left) and B (right). Reproduced with permission.[14] Copyright 2015, Heim

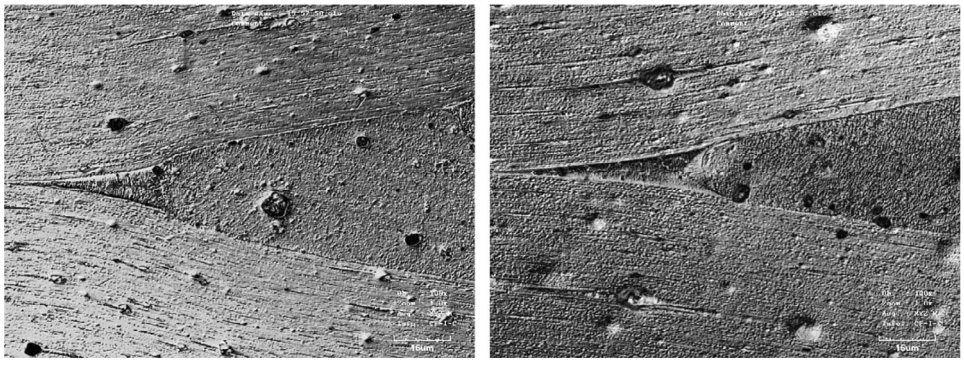

FIGURE 5 Detailed reflected light images of the CLSM with ×1000 magnification of wet chemically etched, self-reinforced composites structures made of SG30/30 according to the process parameters A (left) and B (right). Reproduced with permission.[14] Copyright 2015, Heim

compaction in Process A was insufficient. The sample cross section was examined in addition to the microscopic examinations. It was examined at four different points of the manufactured laminate with three repeated measurements using micrometre screw. A composite thickness of $t_{SNW17,A} = 1.8375$ mm with a standard deviation of $SD_{SNW17,A} = 0.028$ was recorded for the samples manufactured according to process A. Samples manufactured according to process B were minimally thinner and displayed a composite cross section equalling $t_{SNW17,B} = 1.8225$ mm with a standard deviation of $SD_{SNW17,B} = 0.043$. Advanced density experiments with gravimetric density measurements using the buoyancy method were not performed. In the previous examinations, we were able to determine that the informative value of the results must be viewed critically.[14] This is due to the fact that larger or smaller volumes of air are in the according substrate, causing a wider distribution of the results. Lastly, it is important to note that differing circularities result for the fibre cross sections when observing Figure 4 in correlation with processes A and B. It is evident that (process A) has a higher degree and (process B) a lower degree of roundness in the fibre cross section, which correlates with the fibre cross sections. In order to be able to perform an informative, quantitative analysis here, the variables of the image sections shown here are not sufficient. The measurement of circularities and fibre cross sections was focused upon in a different experimental series performed on this material system across the entire laminate cross section, and showed, depending on the degree of compaction, diverging fibre diameters for D_{SNW17} between 24.7 and 28.8 µm, consistent with circularities of fibre filaments C_{SNW17} ranging between 0.5 and 0.67.[14]

4.2 | Structural description of the composites made of the mono-extruded twill fabric SG30/30

The detailed images of the fabric-based layered composites made of SG30/30 in Figure 5 show tape structures with textures analogous to their directions of stretching (= and ⊥ to the image plane).

The composites made with the mono-extruded tape system SG30/30 display less textural distinctions regarding the composite topology. The visible primary orientations made it possible to make indirect deductions about the directions of stretching of the cold stretching. Moreover, the superstructures are disrupted by clusters, which, as can be seen in Figure 6, are identifiable as soot particles displaced during the applied sanding and/or wet chemical etching process.

A thermogravimetric analysis (TGA) of the semi-finished textile product confirmed the addition of approximately 1.7 wt-% of soot particles.[36] These soot particles

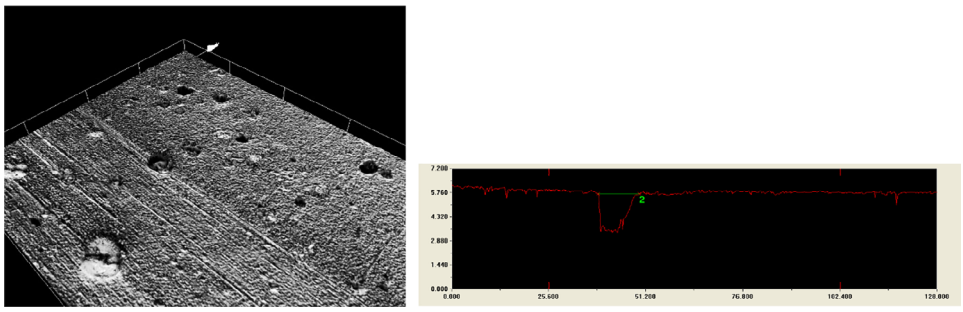

FIGURE 6 3D measurement of soot particle error site with a diameter of 10.75 µm on the surface of an SG30/30 composite sample made using process series B. Reproduced with permission.[14] Copyright 2015, Heim [Color figure can be viewed at wileyonlinelibrary.com]

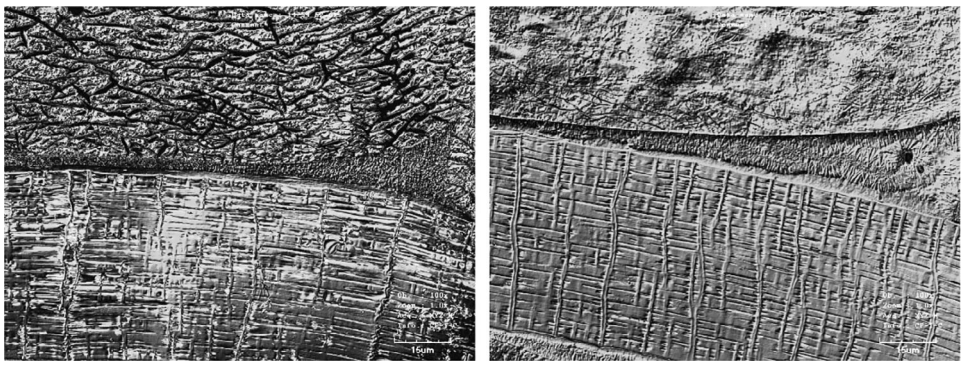

FIGURE 7 Detailed reflected light images of the CLSM with ×1000 magnification of wet chemically etched, self-reinforced composites structures made of Pure according to the process parameters A (left) and B (right). Reproduced with permission.[14] Copyright 2015, Heim

are inherent in the SG30/30 semi-finished fabric products. They were added in order to make the geotextile UV resistant and dye it black for its intended application. The soot particles initiate tear-like breakage of the foil tapes in the longitudinal direction during cold stretching, which was employed during the manufacture of the highly stretched foil tapes. This tear-like breakage is an already known phenomenon that occurs when spinning fibres and is caused by the fracture of disruptive filaments.[41]

4.3 | Structural description of the composite made of the co-extruded canvas fabric pure

The composites made of the co-extruded tape fabric Pure display much more strongly marked superstructures than the mono-extruded material systems, see Figure 7. Clear textural distinctions of the tapes with directions of stretching parallel or orthogonal to the image area are able to be differentiated. Furthermore, marginally extruded border layers are able to be clearly discerned from the highly stretched core layers with a volume ratio of the border layers and core layers (B:C:B) of 5:90:5 determined by structural analysis.[21]

When comparing both processing procedures directly with one another, comparably rougher surface structures of the highly oriented core layers are identifiable for the composite with a lower degree of compaction (process parameter A). This observation could originate from the fact that the lower compaction degree promotes a lower packing density in the polymer morphology. The wet chemical etching was therefore able to achieve stronger etching under identical conditions in process A and remove the amorphous joint structures to a strong degree, ultimately exposing the (highly) oriented structures more significantly.

In case of the tapes of the processing series Process A oriented orthogonal (⊥) to the image plane, there are also fissures in form of plastic depressions to even fine tears, see Figure 7, left, upper half. These can be explained by the low density $\rho_{Pure} = 0.760$ g/cm^3 [14] in the free cavities of the highly stretched film tapes.[42,43]

These so-called free cavities especially occur at high degrees of stretching in foil tapes. During the deformation needed and induced for incorporating large degrees of stretching, (over)stretching of the amorphous regions occurs, causing gliding to occur between the individual lamella blocks depending on the loading scenario, which can lead to a displacement of the crystalline areas.[44] The "joining" amorphous phase is subject to pure shearing deformation, which aligns itself parallel to the lamella surface (in the direction of shearing), and constricts during high tensile loading.[44] Very high stretching degrees can also cause separation of the individual folded blocks. Micro-fibril formation can also occur along with this, and, under certain tension conditions, can tend to cause

free cavities to form.[44] In the case of the hot-compacted SR-PP composite, certain process conditions can also cause plastic depressions to even fine tears.

The textural characteristics of the composite with the higher degree of compaction (process parameter B) suggest a comparably "closed" state of the surface topology. The surface roughness is less pronounced. It can be assumed that the previously mentioned cavities were, for the most part, sealed due to the exposure to the high temperature, which is also evident in the higher density. Moreover, the transcrystalline re-crystallization of the co-extruded marginal layers was more strongly pronounced in comparison to process series A.

After exposure to the high temperature in the hot compaction process, they re-crystallize back to one-dimensionally oriented transcrystalline growth fronts owing to their steric impairment. Transcrystallization has been known of for polymers since the early 1950s.[45,46] The epitaxial growth[47] develop because the nucleation rate at the marginal layers (of for example fibres[48] and injection moulds[49]) is significantly higher than in the actual polymer melt.[46] In this case, the nucleus grows vertical to the inner marginal layers of the core layers to the outer marginal layers of two tapes that run into each other, as was already proven for the UHMWPE fibres embedded in the HDPE matrix.[50]

The development of transcrystallization is strongly influenced by the processing temperatures and the recrystallization conditions. For this reason, the morphological observations will focus upon the composites from process parameter B that were only manufactured with higher processing temperatures (Table 2) and an additional image section is presented in Figure 8.

The characteristics of the one-dimensional growth fronts were very remarkable, and, upon closer observation, it became clear that they develop in correlation with the direction of stretching. The re-crystallized marginal layers of the tapes oriented orthogonally to the image plane displayed significantly clearer definitions of the individual transcrystals than the marginal layers with tapes oriented parallel to the image plane. This is likely due to the fact that epitactically crystallized fold lamellae of the kebab structures located in the highly stretched core areas promote a "plate-shaped" orientation of the transcrystals in the primary direction by means of a nucleation indication.

5 | CONCLUSION

The images made with reflected light microscopy of the self-reinforced polypropylene composites were characterized by the morphology specific for semi-finished textile products. They all shared one common trait, namely that differences regarding the degree of compaction were able to be verified. However, this knowledge cannot simply be transferred to all self-reinforced polypropylene composites in general. Instead, the characteristics that can be derived from the morphological structures of the semi-finished textile products must be determined, analysed independently from the according basic material, and must be described while taking the composites into account.

The composite made from the *needle-punched staple fibre fleece SNW17* was characterized by a low degree of compaction with air enclosures that resulted from insufficient compaction. In contrast, the higher the degree of compaction selected for the fibre-based semi-finished textile product, the less circular the individual fibre filaments in the later composite. Thus, it can be stated that air enclosures and the circular shape of pressure-sensitive fibre filaments can be referenced as structural characteristics of fibre fleeces in order to describe the degree of compaction.

In the composites made from tape fabric, no enclosures of air or other cavities were detected. This allows one to deduct that a sufficient degree of compaction was able to be achieved during hot compaction while using a

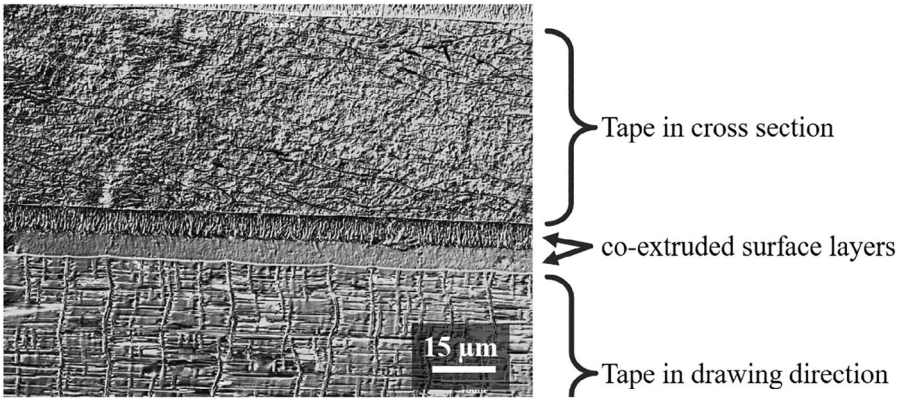

FIGURE 8 Confocal laser scanning microscopy analysis of the composite topology; surface treatment wet chemical etching. Tape in cross section is orthogonal to the image plane, tape in drawing direction is parallel to the image plane. Reproduced with permission.[14] Copyright 2015, Heim

relatively low temperature and pressure. Filling materials, such as mixed in soot particles, were visible as superstructures and show the stretching direction of the tapes, as was verifiable for the black tape fabric of the *SG30/30 composites*. In case of the *Pure composites*, the marginal layers and core layers were visible separately in both process series A and B, and were characterized by the sample with the lower degree of compaction displaying a rougher surface topology, especially in tapes stretched orthogonally to the image plane. The influence of the degrees of compaction can be identified by the roughness or the fissured surface structures.

ACKNOWLEDGMENTS

This article is based on investigations carried out in my doctoral thesis. I would like to express my gratitude to Prof. Dr.-Ing. Hans-Peter Heim, my PhD supervisor, as well as colleagues and students of the Institute for Materials Engineering at the University of Kassel for their support. Open access funding enabled and organized by Projekt DEAL.

ORCID

Angela Ries https://orcid.org/0000-0003-4766-2389

REFERENCES

[1] L.M. Morgan, B.M. Weager, C.M. Hare, G.R. Bishop, G.M. Smith, Proc. 17 Conf. Compos Mater. **2009**, *5*, 13.
[2] B. Pornnimit, G. W. Ehrenstein, *Adv. Polym. Tech* **1991**, *11*, 91.
[3] G. W. Ehrenstein, *Polymer Werkstoffe*, Carl Hanser Verlag, München, Germany **1999**.
[4] Bjekovic, R., Dissertation, University of Kassel, **2003**.
[5] J. Klimke, *Kunststoffe* **2002**, *92*, 45.
[6] P. J. Hine, I. M. Ward, N. D. Jordan, R. H. Olley, D. C. Bassett, *Polymers* **2003**, *44*, 1117.
[7] N. D. Jordan, D. C. Bassett, R. H. Olley, P. J. Hine, I. M. Ward, *Polymers* **2003**, *44*, 1133.
[8] M. A. El-Maaty, D. C. Bassett, R. H. Olley, P. J. Hine, I. M. Ward, *J. Mater. Sci* **1996**, *31*, 1157.
[9] P. J. Hine, I. M. Ward, *J. Appl. Polym* **2006**, *101*, 991.
[10] P. J. Hine, I. M. Ward, N. D. Jordan, R. H. Olley, D. C. Bassett, *J. Macromol. Sci. B* **2001**, *40*, 959.
[11] I. M. Ward, P. J. Hine, *Polymers* **2004**, *45*, 1413.
[12] A. K. Bledzki, H.-P. Heim, D. Paßmann, A. Ries, in *Synthetic Polymer-Polymer Composites* (Eds: D. Bhattacharyya, F. Stoyko), Carl Hanser Verlag, Munich, Germany **2012**.
[13] Á. Kmetty, T. Bárány, J. Karger-Kocsis, *Prog. Polym. Sci.* **2010**, *35*, 1288.
[14] A. Ries, Dissertation, University of Kassel, **2015**.
[15] B. Alcock, N. O. Cabrera, N.-M. Barkoula, C. T. Reynolds, L. E. Govaert, T. Peijs, *Compos Sci Technol* **2007**, *67*, 2061.
[16] B. Alcock, N. O. Cabrera, N.-M. Barkoula, Z. Wang, T. Peijs, *Compos. B. Eng.* **2008**, *39*, 537.
[17] T. N. Abraham, S. D. Wanjale, T. Bárány, J. Karger-Kocsis, *Compos. Part A Appl. Sci. Manuf.* **2009**, *40*, 662.
[18] S. McKown, W. J. Cantwell, *J. Compos. Mater* **2007**, *41*, 2457.
[19] G. Romhany, T. Barany, T. Czigany, J. Karger-Kocsis, *Polymer Adv Tech* **2006**, *18*, 90.
[20] A. K. Bledzki, D. Passmann, A. Ries, A. Chate, *Mater. Test* **2008**, *50*, 623.
[21] Passmann, D., Dissertation, University of Kassel, **2009**.
[22] M. Duhivic, S. Fakirov, R. Holschuh, P. Mitschang, D. Bhattacharyya, in *Synthetic Polymer-Polymer Composites*, Vol. 1 (Eds: D. Bhattacharyya, S. Fakirov), Hanser, München, Germany **2012**.
[23] D. Depla, S. Mahieu, *Reactive Sputter Deposition*, Springer, Berlin Heidelberg New York **2008**.
[24] N. N.: Technical Data Sheet: **2006** SNW, BONAR Technical Fabrics, Belgium, 1 December 2006.
[25] N. N.: Technical Data Sheet: **2008** SG30/30, BONAR Technical Fabrics, Belgium, 25 December 2008.
[26] N.N.: Technical Data Sheet, Pure, Lankhorst, NL-8600 AE Sneek—Netherlands.
[27] M. McKay, W. Conover, R. Beckman, *Technometrics* **1979**, *21*, 239.
[28] M. Hou, K. Friedrich, *J Mater Sci Mater Med* **1998**, *9*, 83.
[29] B. P. Kremer, H. Bannwarth, *Einführung in die Laborpraxis*, Springer-Verlag, Berlin Heidelberg, Germany **2011**.
[30] N. N., Software für konfokales Laser-Scaning-Mikroskop Lext OLS3100 Oberflächentextur-Analyse in der dritten und vierten Dimension, Hanser Verlag, QZ-online, 7 January 2009. **2009**.
[31] M. Kern, J. Trempler, *Beobachtende und messende Mikroskopie in der Materialkunde*, Brünne-Verlag, Berlin, Germany **2007**.
[32] M. Maas, *QZ* **2005**, *50*, 108.
[33] A. Breining, G. W. Ehrenstein, J. Varga, *Materialprüfung* **1997**, *39*, 81.
[34] A. Breining, Dissertation, University Erlangen-Nürnberg, **2005**.
[35] Z. Bashir, M. J. Hill, A. Keller, *J. Mater. Sci* **1986**, *5*, 876.
[36] H.-P. Heim, A. Ries, B. Rohde, *AIP Conf. Proc.* **2014**. *1593*, 776. https://doi.org/10.1063/1.4873890.
[37] R. H. Olley, *Sci. Prog.* **1986**, *70*, 17.
[38] R. H. Olley, D. C. Bassett, *Polymer* **1982**, *23*, 1707.
[39] L. C. Sawyer, D. T. Grubb, G. F. Meyers, *Polymer Microscopy*, Springer Science+Business Media, NY, USA **2008**.
[40] A. Garton, D. J. Carlsson, D. M. Whes, *Text. Res. J.* **1978**, *48*, 115.
[41] B. Becker, R. Schulte, J. Winkler, M. Wedler, I. Reinhard, A. Claßen, *German patent application DE10118704A1*, **2002**.
[42] P. J. Hine, V. Broome, I. M. Ward, *Polymer* **2005**, *46*, 10936.
[43] B. Alcock, N. O. Cabrera, N.-M. Barkoula, A. B. Spoelstra, J. Loos, T. Peijs, *Compos Pt A Appl. Sci. Manuf.* **2007**, *38*, 147.
[44] S. Rettenberger, Dissertation, Friedrich-Alexander-Universität Erlangen-Nürnberg, **2002**.
[45] E. Jenkel, E. Teege, W. Hinrichs, *Kolloid-Zeitschrift* **1952**, *129*, 19.
[46] B.-J. Jungnickel, *Transkristallisationsneigung metallocen-katalysierter Polypropylene*, Zusammenfassung AiF-Nr.: 12946 N.
[47] H.-G. Elias, *Makromoleküle: Industrielle Polymere und Synthesen*, Wiley, Weinheim, Germany **2003**.
[48] C. Wang, C.-R. Liu, *Polymers* **1999**, *40*, 289.

[49] M. Bonnet, *Kunststoffe in der Ingenieuranwendung: verstehen und zuverlässig auswählen*, Vieweg + Teubner, GWV Fachverlag GmbH, Wiesbaden, Germany **2009**.

[50] H.-J. Kestenbach, J. Loos, J. Petermann, *Mater. Res* **1999**, *2*, 261.

How to cite this article: A. Ries, *J Appl Polym Sci* **2021**, *138*(41), e51215. https://doi.org/10.1002/app.51215